Conductance of a copper-nanotube bundle interface: Impact of interface geometry and wave-function interference

Steven Compernolle,[1,2,*] Geoffrey Pourtois,[2] Bart Sorée,[2] Wim Magnus,[2,3] Liviu F. Chibotaru,[1] and Arnout Ceulemans[1]
[1]*Laboratorium voor Kwantumchemie and Institute for Nanoscale Physics and Chemistry (INPAC), Katholieke Universiteit Leuven, Celestijnenlaan 200F, B-3001 Heverlee, Belgium*
[2]*Interuniversity MicroElectronics Centre (IMEC), Kapeldreef 75, B-3001 Heverlee, Belgium*
[3]*Department of Physics, Universiteit Antwerpen, Groenenborgerlaan 171, 2020 Antwerpen, Belgium*
(Received 15 September 2007; revised manuscript received 29 February 2008; published 20 May 2008)

Carbon nanotubes (CNTs) are a promising candidate to replace copper interconnects. An *ab initio* study is presented on the conductance of a closed-packed *bundle* of very narrow metallic (4,0) CNTs, which is vertically placed on a Cu (100) surface. The intertube interactions have no significant impact on the conductance. The conductance is highly dependent on the exact geometry of the interface, which is varying between 0.6 and 1.8 conductance quanta, while the theoretical maximum of the CNT is three conductance quanta. The wave-function interference can lead to conductance suppression when the packing is too high. Both features are explained by using an orbital picture.

DOI: 10.1103/PhysRevB.77.193406 PACS number(s): 73.22.−f, 73.23.Ad, 73.40.Cg, 73.40.Jn

I. INTRODUCTION

The conductance of a metal-carbon nanotube (metal-CNT) system is the subject of intensive research, both experimentally[1–4] and theoretically by *ab initio* calculations.[5–14] One of the great challenges of the field is to get the contact resistance as low as possible. The *ab initio* studies provide a wide range of varying values for the conductance of metal-CNT systems, which originates from different choices in the model, such as the kind of metal [Al,[5–11] Au,[1,5,6,15] Ti,[2,6,13,14] or Pd (Refs. 4, 13, and 15)], the nature of the contact (side contact,[6,11] end contact,[5–10,12,14] or embedded contact[13,15]), and the type of carbon nanotube (CNT) (armchair[6,7,10,11,13–15] or zigzag[8,9]).

Presently, Cu is widely used as an interconnect. However, when the dimensions of the interconnect become too small, the resistivity increases by scattering through the surface defects and grain boundaries.[16] The metallic carbon CNTs are one possible alternative since they have a long mean free path and can conduct much larger current densities than copper wires. A recent study showed that for the highest performance, the CNTs should be vertically placed on the metallic surface, which is single wall and is as thin and as closely packed as possible.[16] However, it was assumed that the bundling and narrow diameters have no impact on the performance per CNT. To the best of our knowledge, an *ab initio* investigation on the conductance of such a closed-packed *bundle* of ultranarrow CNTs on a metal has not been investigated yet; instead, the focus was always on the isolated CNTs.

We choose Cu for the metal, as it is one of the most important materials in microelectronics, and Cu-CNT integrated interconnects can be a viable alternative to a total replacement of Cu interconnects.[16]

II. STRUCTURES AND METHOD

The thinnest experimentally observed CNT is ~3 Å in diameter,[17] which corresponds to a (2,2) armchair, (3,1) chiral, or (4,0) zigzag CNT. The simple zone-folding method (ZFM) rules[18] to determine metallicity do not generally hold for very narrow CNTs. While ZFM predicts the (2,2) CNT to be a metal and the (3,1) and (4,0) CNTs to be semiconductors, the *ab initio* density functional theory (DFT) studies[19] reveal that the first one is an indirect semiconductor, the second is a semiconductor, and the last one is a metal. Since for interconnects we are obviously interested in the metallic CNTs, the (4,0) CNT is chosen. For Cu, the (100) surface is taken.

As was illustrated for an Al-CNT system,[9] the conductance will also depend on the exact geometry of the end contact. Hence, we choose four different geometries of the Cu-CNT contact with C_{4v} symmetry, which are labeled as Figs. 1(a)–1(d).

We define two periodic CNT arrays, with one CNT per two-dimensional unit cell and with this unit cell, a multiple of the Cu (100) surface unit cell (Fig. 2). The lattice vectors of Cu (100) are $\mathbf{L}_{\mathrm{Cu},1}=L_{\mathrm{Cu}}(\mathbf{e}_x+\mathbf{e}_y)$ and $\mathbf{L}_{\mathrm{Cu},2}=L_{\mathrm{Cu}}(\mathbf{e}_x-\mathbf{e}_y)$, where $L_{\mathrm{Cu}}=2.523$ Å. The lattice vectors of the first CNT array are $\mathbf{L}_{a,1}=4\mathbf{L}_{\mathrm{Cu},1}$ and $\mathbf{L}_{a,2}=4\mathbf{L}_{\mathrm{Cu},2}$ with a packing of one CNT/S_a, where $S_a=16L_{\mathrm{Cu}}^2\approx 101.85$ Å,[2] while those of the second are $\mathbf{L}_{b,1}=2\mathbf{L}_{\mathrm{Cu},1}+2\mathbf{L}_{\mathrm{Cu},2}$, $\mathbf{L}_{b,2}=2\mathbf{L}_{\mathrm{Cu},1}-2\mathbf{L}_{\mathrm{Cu},2}$ with a packing of two CNT/S_a or one CNT/S_b, where $S_b=\mathrm{S}_a/2$. The smallest distance between two CNT walls is 6.8 Å in the first case and 4.0 Å in the second.

First, we make a guess of the distance between the CNT and the Cu surface by rigidly changing the Cu-CNT distance and taking the structure with the lowest total energy. The relaxation of the interface atoms is performed with the software package SIESTA,[20] which combines DFT, finite-range atomic orbitals, and three-dimensional periodic boundary conditions. We use the local density approximation with optimized pseudopotentials and double zeta with polarization basis sets, which are developed by the simplex method.[21] Upon relaxation, the Cu-CNT distance did not appreciably change anymore.

The package ATOMISTIX TOOLKIT (ATK),[22] which is based on DFT and nonequilibrium Green's functions, is used to

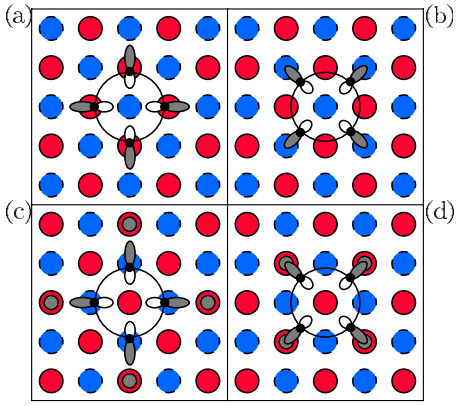

FIG. 1. (Color online) Schematic picture of the four geometries of a Cu-CNT interface studied in this work. The large black circle indicates the CNT. Small black circles: first atoms of the CNT, with their $2p\pi$ orbitals (gray-white lobes) indicated. Large red circles, solid line: Cu atoms of the first layer; only the $4s$ orbitals of (gray circles) Cu efficiently interacting with the $2p\pi$ orbitals are shown. Large blue circles dashed: Cu atoms of the second layer. (a) The first four atoms of the (4,0) CNT are on top of the four atoms of the first Cu layer. (b) The CNT is rotated 45° with respect to (a). (c) The first four atoms of the (4,0) nanotube are located above the four atoms of the second Cu layer. (d) The nanotube is rotated 45° with respect to (c). Only for structures (c) and (d) is an efficient interaction possible between $2p\pi$ orbitals of the CNT and $4s$ orbitals of the Cu surface.

calculate the transport properties. In ATK, the structure is divided into two half-infinite electrodes, in our case Cu and the (4,0) CNT array, where the geometry and electron density are assumed to be the bulk value and the central region. The central region consists of four Cu layers and two CNT unit cells. The same functional and pseudopotentials are used as for the SIESTA calculations. However, due to the high computational cost of the transport calculations, we confine ourselves to the default single zeta (SZ) and double zeta (DZ) basis sets provided by ATK, and performed no structure relaxations within ATK. Since the trends for the ideal and relaxed geometries, and for SZ and DZ basis sets are the same, we only present here the results for SZ and ideal geometries, for which we have the full data set. For comparison with the interface structures, we have also performed transport calculations for the perfect periodic CNT arrays with packings for one CNT/S_a and two CNT/S_a, and for Cu.

The zero-bias conductance is given by

$$G = G_0 \int_{-\infty}^{+\infty} \left[\frac{df(E)}{dE} \sum_j \frac{S}{4\pi^2} \int_{\mathrm{FBZ}} T_{j,\mathbf{k}}(E) d\mathbf{k} \right] dE$$

$$= G_0 \int_{-\infty}^{+\infty} \bar{T}(E) dE, \qquad (1)$$

where $G_0 = 2\frac{e^2}{h}$ is the conductance quantum and $f(E)$ is the Fermi-Dirac distribution. As the system is periodic in x and y, the conductance involves an integration over a two-dimensional first Brillouin zone (FBZ). j counts the contributing conduction channels (CCs). $\bar{T}$ is the total transmission

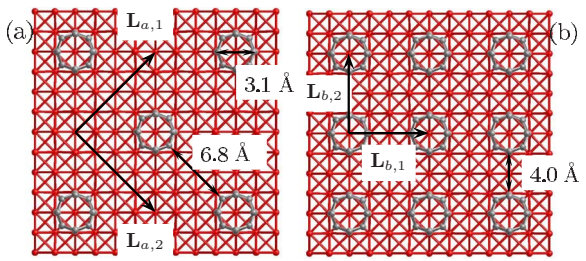

FIG. 2. (Color online) Top view of a Cu-CNT array interface [with the geometry of Fig. 1(d)] with a packing of (a) one CNT/S_a and (b) two CNT/S_a. C atoms are gray and Cu atoms are red. The vectors $\mathbf{L}_{a,1,2}$ and $\mathbf{L}_{b,1,2}$ define the periodic boundary conditions in the x and y directions.

for an area S. The use of one-dimensional electrodes (such as CNTs) in the Landauer-Büttiker formulation has been criticized,[23] but we have argued[24] that it is justified provided that only zero-bias conductances are calculated.

III. RESULTS

We first discuss the conductance of the ideal, infinite electrodes. For a packing of one CNT/S_a, there is no significant interaction between the CNTs; this is illustrated by the integer $\bar{T}$/CNT [Fig. 3(a)]. The transmission of three [Fig. 3(a)] in a wide region around the Fermi level E_F is in contrast to the wide-diameter metallic CNTs for which it is only two. In agreement with this, the band structure of the small-diameter CNTs can be radically different from those of their wide-diameter counterparts.[19] For a packing of two CNT/S_a, the CNTs do feel each other, as the $\bar{T}$/CNT is a noninteger in general [Fig. 3(a)]. However, around E_F, it is still an integer and equal to three, which suggests that intertube coupling is not important at E_F. This is again in contrast to the wide-diameter CNTs, where the intertube coupling directly lowers the transmission at E_F.[25] The underlying principle for this effect is well known. The metallic character of a wide-diameter nanotube finds its origin in the crossing of two symmetry distinct bands. When considering a bundle of interacting nanotubes, those bands are no longer symmetry distinct and the two bands repel, leading to a pseudogap[25] (pseudo as the repellation does not occur over the entire Brillouin zone). For the (4,0) nanotube, the situation is different. The bands causing metallicity are parabolic in nature and nanotube interaction will not lead to a gap opening.

The number of conduction channels by itself does not lead to the conductance of the interface structure. However, it does provide us with an upper limit. In this sense, the (4,0) CNT has a higher potential than a standard wide-diameter metallic CNT. $\bar{T}$ of the Cu electrode per area $S_a/2$ varies between seven and nine over a wide region around E_F (data not shown). Hence, even in the case of a very high packing of two CNT/S_a, the Cu electrode has considerably more wave functions available for transport than the CNT array. This suggests that $\bar{T}$ of the interface will be more sensitive to variations of $\bar{T}$ of the CNT array electrode rather than that of the Cu electrode.

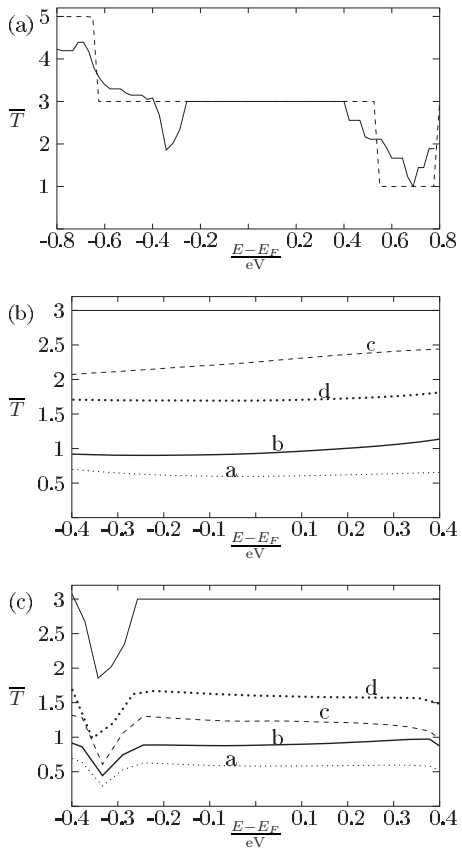

FIG. 3. (a) Dashed line: $\bar{T}$/CNT for a CNT array with one CNT/S_a. Solid line: $\bar{T}$/CNT for a CNT array with two CNT/S_a. (b) $\bar{T}$/CNT of the Cu-CNT array interfaces with one CNT/S_a and with the interface geometries as defined in Figs. 1(a)–1(d). The upper solid line is the $\bar{T}$/CNT for the infinite CNT array. (c) Same as (b), but now with two CNT/S_a.

Let us now consider the conductance of the interfaces. For a packing of one CNT/S_a, the $\bar{T}$/CNT at E_F are 0.6, 0.9, 1.7, and 2.3 for the four interface geometries [Fig. 3(b)], or about 20, 30, 57, and 77 percent, respectively, of the total conductance capacity of the CNT array. Also, the $\bar{T}$ is almost constant around E_F, which reflects the perfectly constant $\bar{T}$/CNT of the infinite CNT array. Note also that for the structure in Fig. 1(c), the conductance is higher than $2G_0$, which is the upper limit for standard metallic CNTs. In principle, this shows that higher number of conduction channels can be beneficial.

The difference between the four interface geometries can be understood from an orbital model. The wave functions of the CNT have a $2p\pi$ character, while that of Cu have $3d$ and $4s$ characters. Let us assume that the main transmission across the interface happens through $2p\pi$ and $4s$ orbital overlaps. Thus, the wide variation in $\bar{T}$ can readily be understood. For the two interface geometries with the lowest $\bar{T}$, no large $2p\pi$-$4s$ interactions are possible; the Cu atoms are either too far away from the C atoms, or the $4s$ orbitals are located near the nodes of the $2p\pi$ orbitals. For the two interface geometries with the highest $\bar{T}$, however, four good

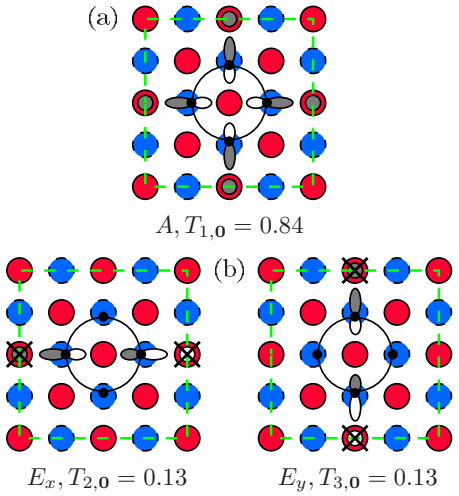

FIG. 4. (Color online) Schematic picture of the interaction between the $2p\pi$ orbitals of the CNT and the $4s$ orbitals of Cu for the interface geometry as defined in Fig. 1(c) and with a packing of two CNT/S for the CCs with $T_{j,0}$, $j=1-3$. (a) A representation: the wave function is even under the rotation of the principal C_2 axis. A good $2p\pi$-$4s$ interaction is possible. (b) Degenerate E representation: the wave function is odd under rotation of the principal C_2 axis; the indicated $4s$ orbitals should be of opposite sign. Taken together with the periodic boundary conditions, this implies that some $4s$ orbitals cannot exist (indicated by a black cross), thereby preventing the $2p\pi$-$4s$ interaction.

$4s$-$2p\pi$ interactions are possible. To examine our hypothesis, we have analyzed the wave functions of the finite CNT on a finite Cu slab inside SIESTA. We find that the $2p\pi$-$4s$ are indeed important for the wave functions that are delocalized over both Cu and CNT.

For a packing of two CNT/S_a, the shape of the $\bar{T}(E)$ curves of the four interface geometries qualitatively have the same shape as that of the infinite CNT array [Fig. 3(c)]; e.g., the dip at −0.35 eV is present for all structures. Quantitatively, they are again widely varying. For three of the four interface geometries, the $\bar{T}(E_F)$/CNT at E_F is almost the same as for the packing of one CNT/S_a, and can be explained by the same arguments of orbital overlap. However, for the one interface geometry, which corresponds to the interface geometry in Fig. 1(c), $\bar{T}(E_F)$/CNT drastically drops from 2.3 to 1.2. We show that this is due to the wave-function interference due to too close packing of the CNTs.

In Fig. 4, a schematic picture of the interaction between the $2p\pi$ orbitals of the CNT and the $4s$ orbitals of Cu is given for the three CCs at the Γ point. The three CCs can be labeled according to group theory: one A representation and a double degenerate E representation. For the A-type CC, a good $2p\pi$-$4s$ orbital interaction is possible. However, this is not the case for the E-type CCs. The combination of an antisymmetric C_2 axis and the periodic boundary conditions forbids the existence of $4s$ orbitals vital for the transmission and, hence, two of the three CCs are strongly suppressed (0.13 each, Fig. 4); the corresponding channels of the system with one CNT/S_a have a much higher transmission of 0.84. Similar arguments apply for the CCs at other k points.

TABLE I. Total energies relative to the most stable structure of the four interface geometries considered in Fig. 1.

Geometry	ΔE_{tot}/eV 1 CNT/S_a	2 CNT/S_a
(a)	1.4	1.60
(b)	2.29	2.69
(c)	1.62	1.62
(d)	0.0	0.0

Hence, the conductance suppression is a pure quantum phenomenon.

Also, the stability of different geometries is directly related to the orbital overlap. Table I reports the total energies of the different interface geometries relative to the most stable one. The geometry of Fig. 1(d) is the most stable, which can be explained by its efficient $2p\pi$-4s interaction.

IV. DISCUSSION AND CONCLUSIONS

Structure relaxations and subsequently transport calculations are done for an interface of Cu (100) and a bundle of very narrow, closely packed metallic (4,0) CNTs. This particular CNT has three transmission channels. Four different interface geometries, all with C_{4v} symmetry, and two packings were studied.

Using the (4,0) CNTs for interconnects over other CNTs has three important advantages: (i) a potentially very dense packing due to its small diameter, (ii) three transmission channels, while most other metallic CNTs have only two, and (iii) no suppression of the transmission at the Fermi level due to intertube coupling. Our study must be seen as a limiting case. The smallest CNTs are also the most fragile, which will make their use difficult. In practice, a compromise has to be made between small diameter and stability.

We find that the conductance is strongly dependent on the interface geometry and explain the difference with an orbital picture model. This model also rationalizes which geometry is the most stable. The intertube interaction itself does not significantly modify the conductance, as the electronic structure of the CNTs is not modified around E_F. However, conductance suppression at high CNT packing can still occur due to destructive interference with the wave functions on the Cu surface and can therefore have a negative impact on the performance of CNT bundles as an interconnect.

ACKNOWLEDGMENTS

Financial support from the Belgian Government through the Concerted Action Scheme (GOA) and the National Science Foundation (FWO-Vlaanderen) is gratefully acknowledged. The authors also thank Atomistix for useful discussions on transport properties.

*Present address: Belgian Institute of Space-Aeronomy, Ringlaan 3, Brussels.

[1] J. Nygard, D. H. Cobden, and P. E. Lindelof, Nature (London) **408**, 342 (2000).
[2] J. Kong, E. Yenilmez, T. W. Tombler, W. Kim, H. J. Dai, R. B. Laughlin, L. Liu, C. S. Jayanthi, and S. Y. Wu, Phys. Rev. Lett. **87**, 106801 (2001).
[3] A. Kanda, K. Tsukagoshi, S. Uryu, Y. Ootuka, and Y. Aoyagi, Microelectron. Eng. **63**, 33 (2002).
[4] D. Mann, A. Javey, J. Kong, Q. Wang, and H. J. Dai, Nano Lett. **3**, 1541 (2003).
[5] J. J. Palacios, E. Louis, A. J. Perez-Jimenez, E. S. Fabian, and J. A. Verges, Nanotechnology **13**, 378 (2002).
[6] J. J. Palacios, A. J. Perez-Jimenez, E. Louis, E. San Fabian, and J. A. Verges, Phys. Rev. Lett. **90**, 106801 (2003).
[7] J. Taylor, H. Guo, and J. Wang, Phys. Rev. B **63**, 245407 (2001).
[8] K. Odbadrakh, P. Pomorski, and C. Roland, Phys. Rev. B **73**, 233402 (2006).
[9] T. Matsumoto and S. Saito, Physica E (Amsterdam) **29**, 560 (2005).
[10] N. Kobayashi, T. Ozaki, and K. Hirose, Physica E (Amsterdam) **29**, 551 (2005).
[11] M. B. Nardelli, J. L. Fattebert, and J. Bernholc, Phys. Rev. B **64**, 245423 (2001).
[12] P. Pomorski, C. Roland, and H. Guo, Phys. Rev. B **70**, 115408 (2004).
[13] N. Nemec, D. Tomanek, and G. Cuniberti, Phys. Rev. Lett. **96**, 076802 (2006).
[14] Y. Liu, Phys. Rev. B **68**, 193409 (2003).
[15] S. H. Ke, W. T. Yang, and H. U. Baranger, J. Chem. Phys. **124**, 181102 (2006).
[16] N. Srivastava, R. Joshi, and K. Banerjee, Tech. Dig. - Int. Electron Devices Meet., 2005, 249 (2005).
[17] L.-M. Peng, Z. L. Zhang, Z. Q. Xue, Q. D. Wu, Z. N. Gu, and D. G. Pettifor, Phys. Rev. Lett. **85**, 3249 (2000); X. Zhao, Y. Liu, S. Inoue, T. Suzuki, R. O. Jones, and Y. Ando, *ibid.* **92**, 125502 (2004).
[18] J. W. Mintmire, B. I. Dunlap, and C. T. White, Phys. Rev. Lett. **68**, 631 (1992); N. Hamada, S. I. Sawada, and A. Oshiyama, *ibid.* **68**, 1579 (1992).
[19] Y. L. Mao, X. H. Yan, Y. Xiao, J. Xiang, Y. R. Yang, and H. L. Yu, Nanotechnology **15**, 1000 (2004); I. Cabria, J. W. Mintmire, and C. T. White, Phys. Rev. B **67**, 121406(R) (2003); V. Barone and G. E. Scuseria, J. Chem. Phys. **121**, 10376 (2004).
[20] J. M. Soler, E. Artacho, J. D. Gale, A. Garcia, J. Junquera, P. Ordejon, and D. Sanchez-Portal, J. Phys.: Condens. Matter **14**, 2745 (2002); P. Ordejon, E. Artacho, and J. M. Soler, Phys. Rev. B **53**, R10441 (1996).
[21] J. Junquera, O. Paz, D. Sanchez-Portal, and E. Artacho, Phys. Rev. B **64**, 235111 (2001).
[22] ATK version 2.0, Atomistix A/S (www.atomistix.com); M. Brandbyge, J. L. Mozos, P. Ordejon, J. Taylor, and K. Stokbro, Phys. Rev. B **65**, 165401 (2002).
[23] Y. Q. Xue and M. A. Ratner, Phys. Rev. B **70**, 205416 (2004).
[24] S. Compernolle, B. Sorée, W. Magnus, and A. Ceulemans (unpublished).
[25] P. Delaney, H. J. Choi, J. Ihm, S. G. Louie, and M. L. Cohen, Nature (London) **391**, 466 (1998).